Ultimate strength of initially deflected plate under longitudinal compression: Part I = An advanced empirical formulation

Do Kyun Kim[1,2 *], Bee Yee Poh[1,a], Jia Rong Lee[1,b] and Jeom Kee Paik[3,4,c]

[1]*Ocean and Ship Technology Research Group, Department of Civil and Environmental Engineering, Universiti Teknologi PETRONAS, 32610 Seri Iskandar, Perak, Malaysia*
[2]*Graduate Institute of Ferrous Technology, POSTECH, 37673 Pohang, Republic of Korea*
[3] *The Korea Ship and Offshore Research Institution (The Lloyd's Register Foundation Research Centre of Excellence), Pusan National University, Busan, Republic of Korea*
[4] *Department of Mechanical Engineering, University College London, London, UK*

(Received keep as blank, Revised keep as blank, Accepted keep as blank) 9pt

Abstract. In this study (Part I), an advanced empirical formulation was proposed to predict the ultimate strength of initially deflected steel plate subjected to longitudinal compression. An advanced empirical formulation was proposed by adopting Initial Deflection Index (IDI) concept for plate element which is a function of plate slenderness ratio (β) and coefficient of initial deflection. In case of initial deflection, buckling mode shape, which is mostly assumed type in the ships and offshore industry, was adopted. For the numerical simulation by ANSYS nonlinear finite element method (NLFEM), with a total of seven hundred 700 plate scenarios, including the combination of one hundred (100) cases of plate slenderness ratios with seven (7) representative initial deflection coefficients, were selected based on obtained probability density distributions of plate element from collected commercial ships. The obtained empirical formulation showed good agreement (R^2 = 0.99) with numerical simulation results. The obtained outcome with proposed procedure will be very useful in predicting the ultimate strength performance of plate element subjected to longitudinal compression.

Keywords: ultimate strength, plate, unstiffened panel, initial deflection, empirical formulation

1. Introduction

Limit state design (LSD), such as ultimate limit state (ULS), fatigue limit state (FLS), accident limit state (ALS), and serviceability limit state (SLS) (Paik 2018), has been growing in emphasis of its importance in recent times. With regards to ULS based design of ships and offshore structures, a number of studies have been conducted in terms of plate element (Paik *et al.* 2008a, ISSC 2012), stiffened panel (Paik *et al.* 2008b, Kim *et al.* 2017, 2018a, Ozdemir *et al.* 2018), and hull girder (Paik *et al.* 2008c, 2013, Park *et al.* 2015a, 2015b). In addition, several researches on ultimate strength of damaged structures by collision (Hogstrom and Ringberg 2012, Jiang *et al.* 2014, Youssef *et al.* 2016), grounding (Paik *et al.* 1998, 2012, Hong and Amdahl 2012, Kim *et al.* 2013a), fire (Guedes Soares *et al.* 2000, Paik et al. 2010, Gordon *et al.* 2011), explosion (Wijaya and Kim 2011, Sohn *et al.* 2013, Czujko and Paik 2015, Kim et al. 2018b, 2018c), dent and local damages (Paik *et al.* 2003, Raviprakash *et al.* 2012, Xu and Guedes Soares 2013, 2015, Witkowska and Guedes Soares 2015), initial imperfection and deformation (Dow and Smith 1984, Guedes Soares 1988, Teixeira *et al.* 2013, Saad-Eldeen *et al.* 2016, Cerik 2018) are also conducted. A wide review of the previous works related to ultimate strength and buckling may be referred to Yao and Fujikubo (2016) and Paik (2018). The more recent studies may also be referred in ISSC (2012, 2015) reports and Paik (2018).

Since the late 19th century, several approaches with various empirical formulations have been proposed. In the early stage, the key concept, called effective width which is used when the deflection occurs by buckling subjected to longitudinal compression, for the plate was raised by John (1987) and approximation technique was adopted by Bortsch (1921). Basically, they tried to evaluate effectiveness of the deflected plate by applied action causing normal stresses corresponding to the identification of plate breadth or width.

In the 20th century, von Karman (1924) proposed the advanced effective width concept by adopting theoretical approaches and effective flange width or effective breadth of simple beams. The von Karman's method was also conducted by Metzer (1929), but for continuous beams instead. A large series of plate testing under compression were also performed by several researchers (Schuman and Back 1930) As of today, several empirical formulations (Box 1883, von Karman 1924, Schnadel 1930, Sechler 1933, Cox 1933, Timoshenko 1936, Marguerre 1937, Frankland 1940, Winter 1940, Chilver 1953, Gerard 1957, BS499 1961, AISC 1964, BS153 1966, Dwight and Moxham 1969, Faulkner 1975, Ueda *et al.* 1975, Carlsen 1977, Ivanov and Rousev 1979, Sereide and Czujko 1983,

*Corresponding author, Senior Lecturer & Adjunct Prof., E-mail: do.kim@utp.edu.my or dokim@postech.ac.kr
[a] Master course student
[b] Engineer
[c] Professor

Hughes 1983, DNV 1987, Smith *et al.* 1988, Ueda *et al.* 1992, Cui and Mansour 1998, Paik *et al.* 2004) have been proposed, which will be covered in Part II (Kim and Poh 2018), with technical review and sensitivity analysis between existing formulations and the obtained advanced formulation based on FE simulation results.

There is, however, still the possibility to improve the accuracy of empirical formulation in predicting ultimate strength of initially deflected plate element subjected to longitudinal compression. Especially, in the range covered by circle shown in Fig. 1, once the ultimate strength performance of plate element by typical empirical formulation, which may be obtained by approximation approach, is suddenly decreased due to the limitation of ultimate strength at material yield strength. However, the behaviour of ultimate strength of plate element tends to decrease smoothly which was obtained by finite element method (FEM) shown in Fig. 1. In addition, the effect of the amount of initial deflection may also affect the ultimate strength of the plate element.

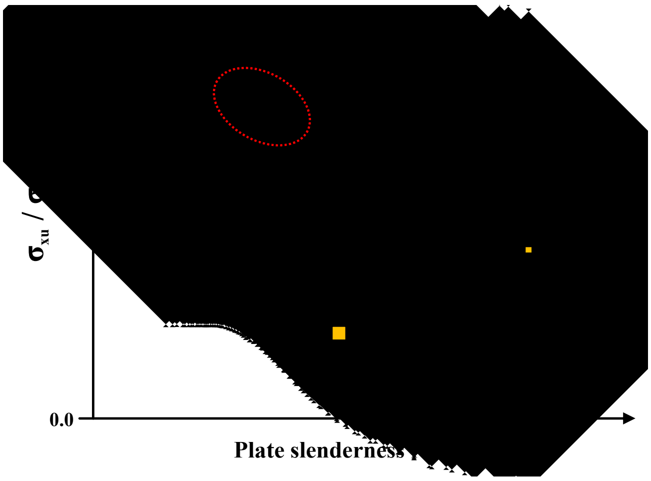

Fig.1 Schematic view of ultimate strength of plate element subjected to longitudinal compression

In this regard, a procedure to propose an advanced empirical formulation is documented in the present paper and the proposed concept was verified by applied example in the present paper (Part I). In addition, an in-depth analysis of the effect of initial deflection on ultimate strength performance of plate element is also taken into account by adopting initial deflection index (IDI) concept proposed in this study.

For the details, a longitudinal compression, which causes the buckling phenomenon due to hull girder bending moment, and different levels of initial deflection are considered in proposing the advanced empirical formulation. For the selection of reliable plate scenarios, three (3) representative midship sections from oil tanker, bulk carrier, and container ships in four (4) different sizes were investigated. In total, twelve (12) midship section data were analysed by probabilistic approaches. Through those probabilistic approaches, reliable plate slenderness ratio, plate width, thickness, and length were obtained. The selected one hundred (100) cases of plate scenarios with seven (7) types of initial plate deflections were employed for the ultimate strength analysis subjected to longitudinal compression. The accuracy of obtained formulation by ANSYS (2014) nonlinear finite element analysis (FEA) was compared with the existing equations.

The complex relation between plate slenderness ratio (β) and coefficient of initial deflection considering buckling mode was also investigated. Throughout the proposed advanced empirical formulation including the technique, structural engineer may easily predict the ultimate strength performance of initially deflected plate element subjected to longitudinal compression.

2. Procedure for the development of empirical formulation

The procedure for the development of advanced empirical formulation, as summarised in Fig. 2, can be directly applied in the prediction of ultimate strength of initially deflected plate element. First, plate data were collected from the representative commercial ships, before the structural characteristics of the plate can be defined in terms of material properties (i.e., plate length, breadth, and thickness) and geometrical properties (i.e., yield strength, Poison ratio, Elastic modulus, etc.). Based on obtained plate information, the plate slenderness ratio (β) can be calculated for all the collected plates. In order to select reliable plate scenarios, the probabilistic identification of selected β is required to be performed as shown in Figs. 3(a) and 3(b). For the efficient and reliable way to select the plate scenarios presented in green coloured box (3rd box from the top) in Fig. 2, the following steps may be recommended to the readers.

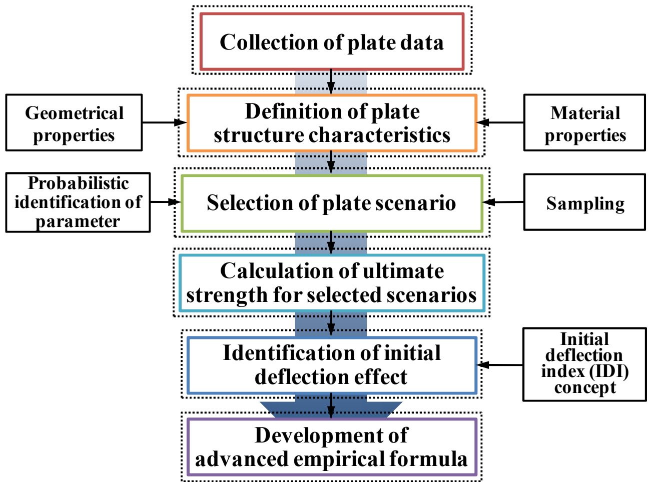

Fig.2 Proposed procedure for the development of empirical formulation

For the selection of the best-fit probability density function (PDF), the goodness-of-fit test for plate slenderness ratio is recommended to be conducted, as shown in Fig. 3(a). Once the best-fit PDF is selected, the best interval can also be found as shown in Fig. 3(b) and 3(c). The area under PDF can then be divided into the required number of plate scenarios. As illustrated in Fig.

3(d), area under the obtained PDF can be divided into ten (10) equal areas if we require ten (10) beta values for the selection of plate scenarios. From each area, beta can also be calculated based on the calculation of centroid into horizontal axis as shown in Fig. 3(d).

The ultimate strength of plate element for the selected scenarios can be calculated by analytical, numerical, and experimental methods. In order to compare the accuracy of the existing methods, especially for the nonlinear FE method, a number of studies with verifications have been conducted by several researchers (ISSC 2012, 2015). In this study, the ANSYS nonlinear finite element method (NLFEM) which is one of the famous numerical simulation codes, is applied to compute the ultimate strength of plate element subjected to longitudinal compression. It is to ensure that other methods may also be applied for the ultimate strength analysis of plate element.

Once the plate scenarios and analysis method are confirmed, the model size and considerable boundary condition should be defined. In general, one-bay and one-span plate model with simply supported condition resulting in slight overestimated outcome is assumed to optimise the computational cost. The detail comparison results on the effect of plate size can be referred to ISSC (2012). In case of initial imperfections, initial deflection and weld-induced residual strength are mostly considered for the numerical simulation. In this study, only the effect of initial deflection by applying buckling mode shape is considered.

Once the ultimate strength analysis is done for the selected reliable plate scenarios, the effect of initial deflection on ultimate strength of plate element can then be established throughout initial deflection index (IDI) concept. Here, initial deflection of the plate was considered as one of the initial damage. The damage index (DI) concept was previously proposed by Paik *et al.* (2012) and has been applied for assessing the safety of oil tankers damaged by grounding by their researcher group. In addition, the concept was also verified by applying on the grounding damaged container ships (Kim *et al.* 2013b) and bulk carriers (Kim *et al.* 2013c) named as a grounding damage index (GDI). Recently, GDI concept was slightly modified to consider the effect of aging-phenomenon by Kim *et al.* (2014). In this study, the initial deflection index (IDI) concept, which can be considered as one of the initial imperfection damage of the plate, is proposed to predict ultimate strength of initially deflected plate element.

The IDI consists of four (4) sub-coefficients; c_1 to c_4 as shown in Eq. (1). In order to consider the effect of initial deflection, an initial deflection coefficient (C_{ID}) with additional three (3) coefficients (= correction coefficient), i.e., ω, ξ, ψ, are required to be adopted, as presented in Eq. (2). Once the ultimate strength analyses of the selected plate are done, three (3) correction coefficients (ω, ξ, ψ) can then be achieved by curve-fitting method. Further details are illustrated in the applied example presented in the next section.

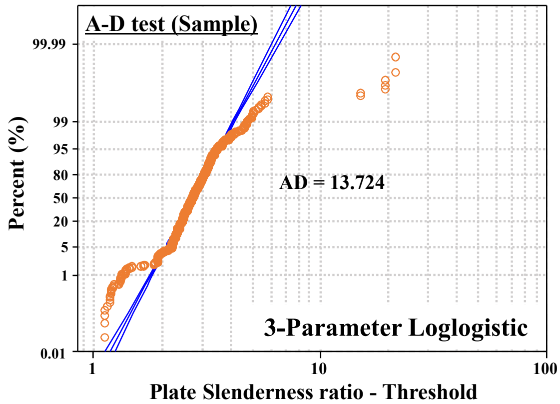

(a) goodness of fit test

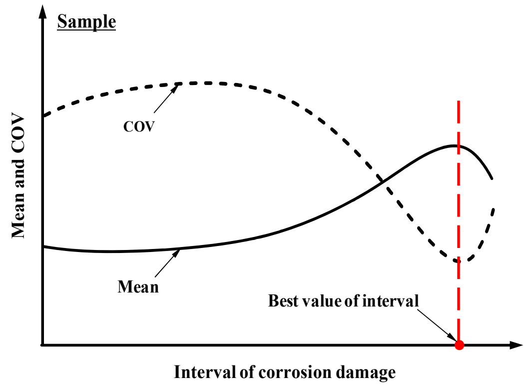

(b) selection of best-interval

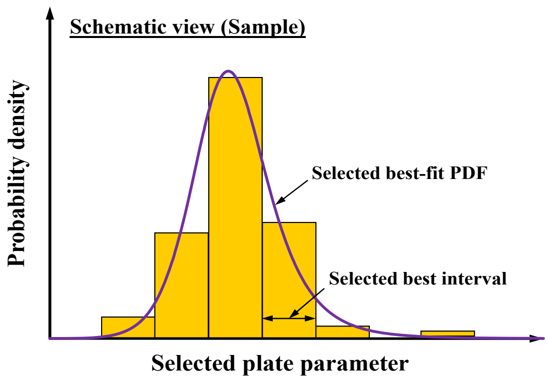

(c) best-fit PDF

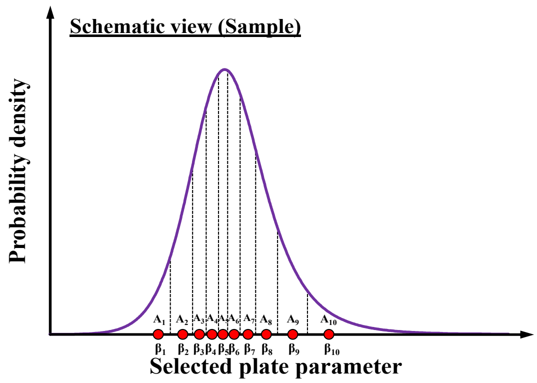

(d) selection of reliable scenarios

Fig.3 Schematic view of probabilistic identification and sampling of selected plate (Note: A = area under PDF, β = plate slenderness ratio, β_i = selected beta)

In the case of initial deflection coefficient (C_{ID}), it can be explained by Eqs. (3) and (4). There are many types of initial deflection shape to be applied to plate element. One of the famous shapes is buckling mode shown in Eq. (3). Previously, Smith *et al.* (1988) proposed three levels of maximum amount of initial deflection such as slight, average, and severe level by assuming hungry horse mode presented. In applying the initial deflection to the plate, buckling mode shape shown in Eq. (3) and (4) is adopted in this study.

$$\mathrm{IDI} = \frac{c_1}{\beta} + \frac{c_2}{\beta^2} + \frac{c_3}{\beta^3} + c_4 \quad (1)$$

$$c_{i,\ i=1\ \mathrm{to}\ 4} = \omega\left(C_{ID}\right)^{\xi} + \psi \quad (2)$$

$$w_{opl} = A_{om} \cdot sin\left(\frac{m\pi x}{a}\right) \cdot sin\left(\frac{\pi y}{b}\right) \quad (3)$$

$$A_{om} = C_{ID} \cdot \beta^2 \cdot t \quad (4)$$

where, IDI = initial deflection index, $\beta = \frac{b}{t}\sqrt{\frac{\sigma_Y}{E}}$, a = plate length, b = plate breadth, t = plate thickness, σ_Y = yield strength, E = elastic modulus, A_{om} = amplitude of the buckling mode initial deflection for longitudinal compressive loading, m = buckling mode half-wave number of the plate in the longitudinal (x) direction which is defined as a minimum integer satisfying $a/b = \sqrt{m(m+1)}$, x = longitudinal direction axis, y = transverse direction axis,

$$w_{opl} = \begin{cases} 0.025\beta^2 t & for\ slight\ level \\ 0.1\beta^2 t & for\ average\ level \\ 0.3\beta^2 t & for\ severe\ level \end{cases}$$

= initial deflection amount of plate proposed by Smith *et al.* (1988).

Based on the obtained ultimate strength performance of plate under longitudinal compression and computed initial deflection index for selected plate scenarios, the ultimate strength versus plate slenderness ratio including the effect of initial deflection, which is called the advanced empirical formulation, can then be proposed as a shape of Eq. (5). The proposed concept will be verified by an applied example in the next section.

Proposed advanced empirical formulation

$$\frac{\sigma_{xu}}{\sigma_Y} = 1 - e^{\mathrm{IDI}} \quad (5)$$

where the IDI is initial deflection index defined in Eq. (1).

3. Applied example

3.1. Collection of plate data & definition of plate structure characteristics

The applicability of the proposed method is verified by an applied example. In total, 3,077 plates with details such as geometrical (plate length, plate breadth, and plate thickness) and material properties (yield strength, elastic modulus, Poison's ratio, etc.) were collected from the 12 representative commercial ship's midship section such as oil tankers (VLCC, Suezmax class, Aframax class, and Panamax class), bulk carriers (181K, 82K, 57K, and 37K) and container ships (13,000TEU, 7,500TEU, 5,000TEU, and 3500TEU) as shown in Figs. 4(a) to (d).

Based on obtained plate information, reliable set of the plate input, i.e., plate length, plate breadth, plate thickness, and plate slenderness ratio are generated in Figs 4(a) to (d) for the investigation of probabilistic characteristics.

3.2. Selection of plate scenario

For the selection of reliable plate scenarios as a prior step, plate slenderness ratio (β), shown in Eq. (6), considered as an important parameter to distinguish plate properties, is computed as presented in Fig. 4(d).

$$\beta = \frac{b}{t}\sqrt{\frac{\sigma_Y}{E}} \quad (6)$$

where, b = plate breadth, t = plate thickness, σ_Y = plate yield strength, E = Young's modulus.

Then, probabilistic identification of each parameter is performed to achieve best-fit probability density functions (PDF) by Goodness of fit test as shown in Figs. 5(a) to (d). In this study, Anderson-Darling test is adopted. Table 1 and Fig. 5 show goodness-of-fit test results for each parameter. In the case of the Anderson-Darling (A-D) test, lowest number represents best-fit probability density function as highlighted in Table 1.

Table 1 Goodness-of-fit test (Anderson-Darling test) for each parameter

	Goodness of fit test (Anderson-Darling)			
Distribution Function	Length (mm)	Breadth (mm)	Thickness (mm)	β
Normal	94.85	632.64	260.02	320.00
Lognormal	149.57	374.44	56.51	112.13
3-Parameter Lognormal	95.12	368.04	25.45	86.51
Exponential	945.93	1043.02	846.55	821.45
2-Parameter Exponential	846.02	1000.19	229.80	754.04
Weibull	98.45	688.07	320.77	380.06
3-Parameter Weibull	94.98	662.83	98.82	346.50
Smallest Extreme Value	286.89	1036.15	654.08	922.95
Largest Extreme Value	176.41	403.23	23.62	116.27
Gamma	128.58	417.86	105.50	118.19
3-Parameter Gamma	105.02	417.28	49.28	116.71
Logistic	**83.26 (Min.)**	234.57	51.05	29.59
Loglogistic	113.76	197.88	13.41	18.09
3-Parameter Loglogistic	83.47	**194.43 (Min.)**	**8.906 (Min.)**	**13.724 (Min.)**

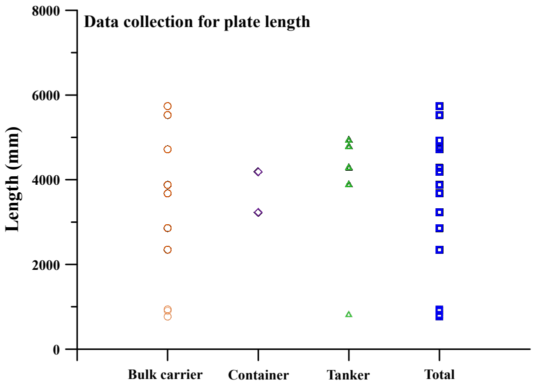

(a) plate length

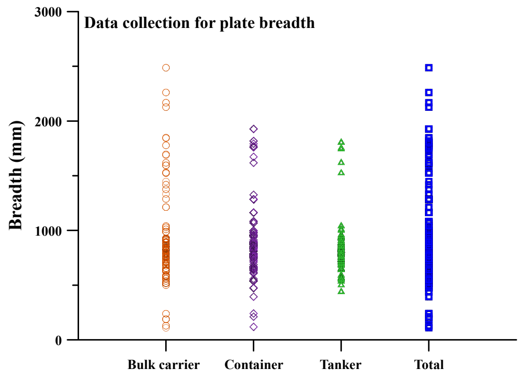

(b) plate breadth

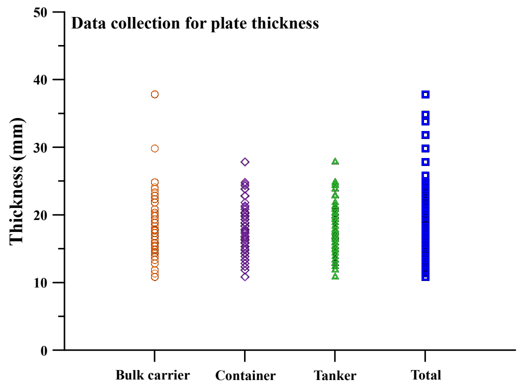

(c) plate thickness

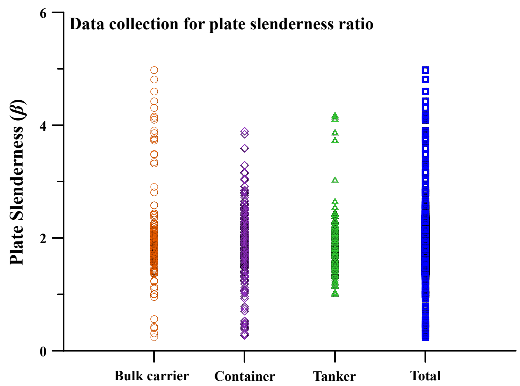

(d) plate slenderness ratio

Fig.4 Collected plate data
(Kim *et al*. 2012a, b, 2013, 2014)

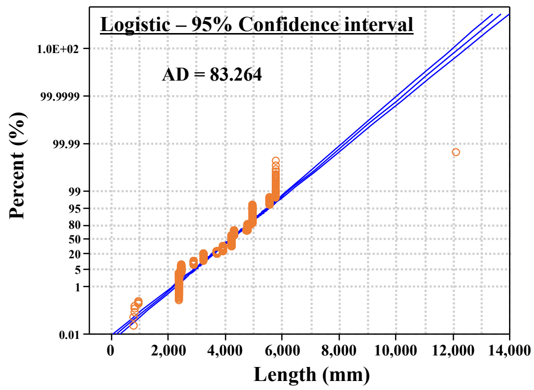

(a) plate length

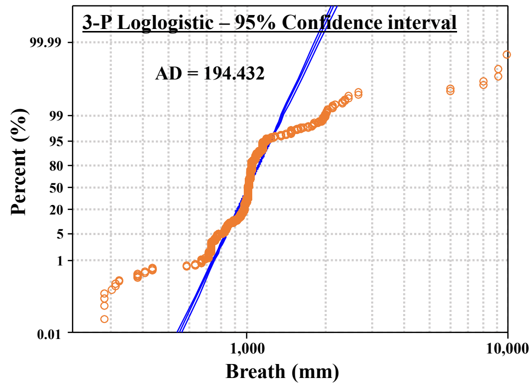

(b) plate breadth

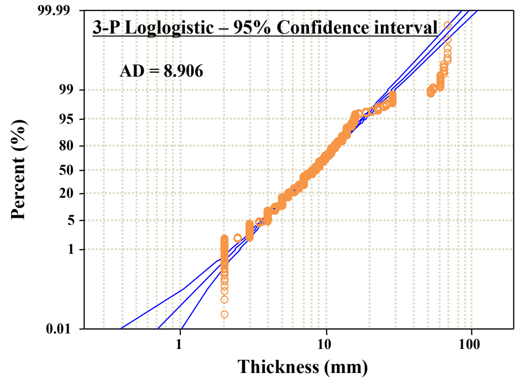

(c) plate thickness

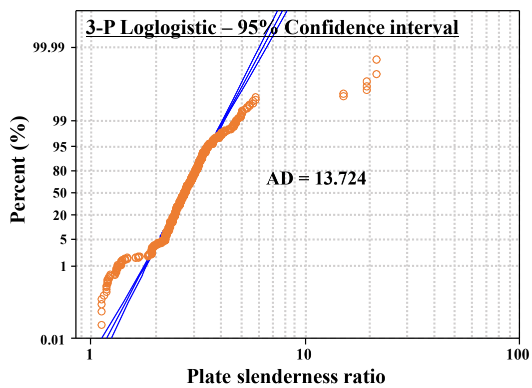

(d) plate slenderness ratio

Fig.5 Goodness of fit test (Anderson-Darling test) for the selection of best-fit probability density functions

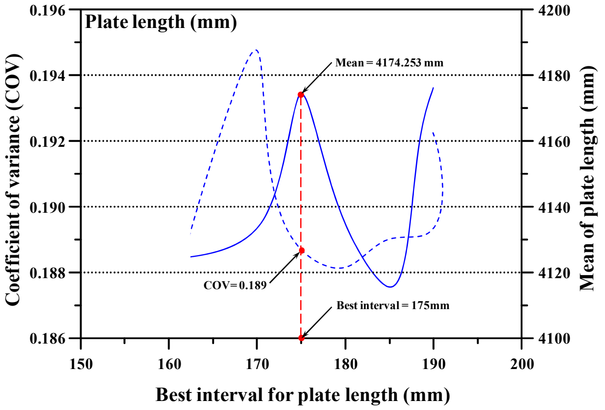

(a) plate length

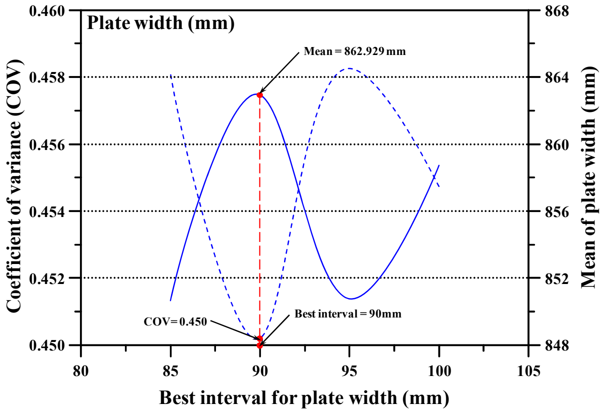

(b) plate breadth

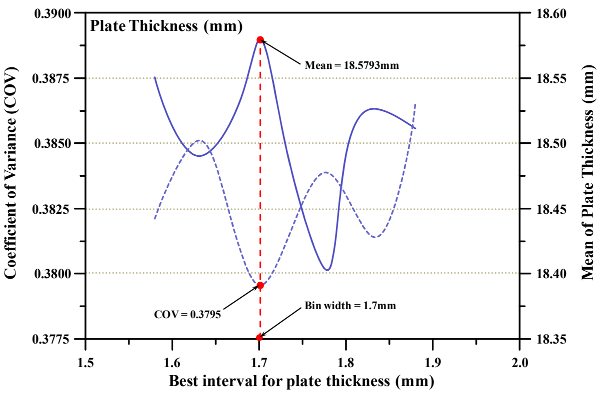

(c) plate thickness

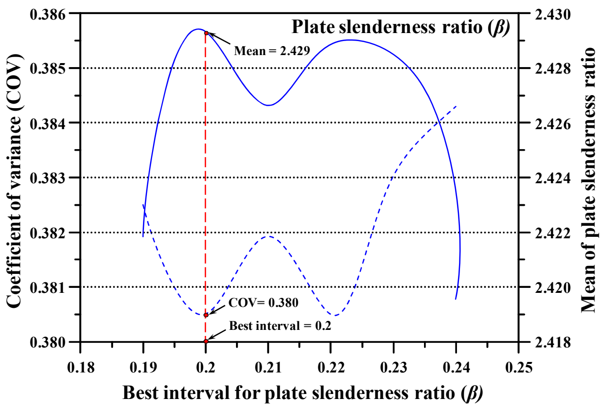

(d) plate slenderness ratio

Fig.6 Selection of best intervals

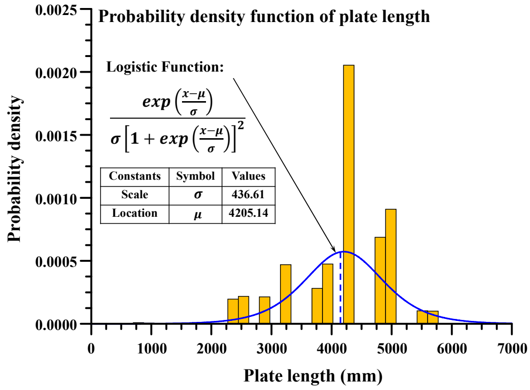

(a) plate length

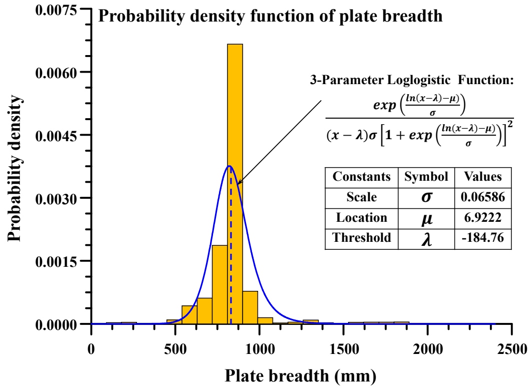

(b) plate breadth

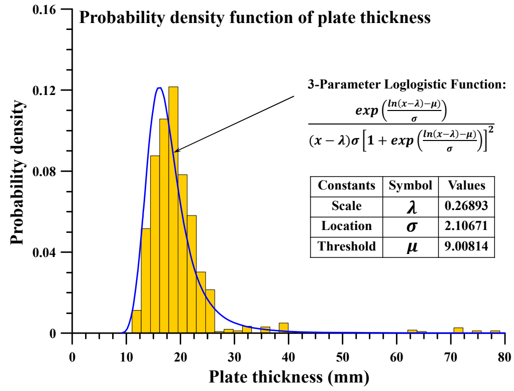

(c) plate thickness

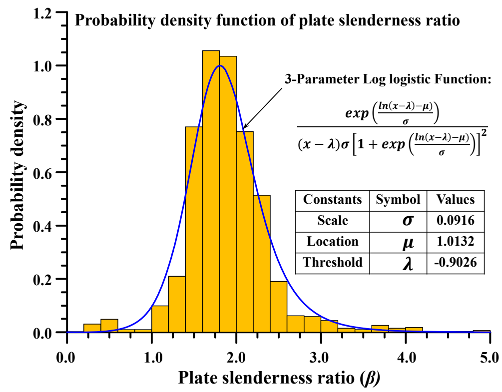

(d) plate slenderness ratio

Fig.7 Obtained best-fit probability density functions

Table 2 Selected plate scenarios

No	a (mm)	b (mm)	t (mm)	σ_Y (MPa)	E (GPa)	β
1	4150	830	44.50	315	205.8	0.73
2	4150	830	38.50	315	205.8	0.84
3	4150	830	36.00	315	205.8	0.90
4	4150	830	34.00	315	205.8	0.96
5	4150	830	32.50	315	205.8	1.00
6	4150	830	31.50	315	205.8	1.03
7	4150	830	31.00	315	205.8	1.05
8	4150	830	30.00	315	205.8	1.08
9	4150	830	29.50	315	205.8	1.10
10	4150	830	29.00	315	205.8	1.12
11	4150	830	28.50	315	205.8	1.14
12	4150	830	28.00	315	205.8	1.16
13	4150	830	27.50	315	205.8	1.18
14	4150	830	27.00	315	205.8	1.20
15	4150	830	26.50	315	205.8	1.23
16	4150	830	26.00	315	205.8	1.25
17	4150	830	25.50	315	205.8	1.27
18	4150	830	25.00	315	205.8	1.30
19	4150	830	24.50	315	205.8	1.33
20	4150	830	24.00	315	205.8	1.35
21	4150	830	23.50	315	205.8	1.38
22	4150	830	23.00	315	205.8	1.41
23	4150	830	22.50	315	205.8	1.44
24	4150	830	22.00	315	205.8	1.48
25	4150	830	21.50	315	205.8	1.51
26	4150	830	21.00	315	205.8	1.55
27	4150	830	20.50	315	205.8	1.58
28	4150	830	20.00	315	205.8	1.62
29	4150	830	19.50	315	205.8	1.67
30	4150	830	19.00	315	205.8	1.71
31	4150	830	18.50	315	205.8	1.76
32	4150	830	18.00	315	205.8	1.80
33	4150	830	17.50	315	205.8	1.86
34	4150	830	17.00	315	205.8	1.91
35	4150	830	16.50	315	205.8	1.97
36	4150	830	16.00	315	205.8	2.03
37	4150	830	15.50	315	205.8	2.09
38	4150	830	15.00	315	205.8	2.16
39	4150	830	14.50	315	205.8	2.24
40	4150	830	14.00	315	205.8	2.32
41	4150	830	13.50	315	205.8	2.41
42	4150	830	13.00	315	205.8	2.50
43	4150	830	12.50	315	205.8	2.60
44	4150	830	12.00	315	205.8	2.71
45	4150	830	11.50	315	205.8	2.82
46	4150	830	11.00	315	205.8	2.95
47	4150	830	10.50	315	205.8	3.09
48	4150	830	10.00	315	205.8	3.25
49	4150	830	9.50	315	205.8	3.42
50	4150	830	8.50	315	205.8	3.82
51	4150	830	42.00	235	205.8	0.67
52	4150	830	36.50	235	205.8	0.77
53	4150	830	34.00	235	205.8	0.82
54	4150	830	32.00	235	205.8	0.88
55	4150	830	30.50	235	205.8	0.92
56	4150	830	29.50	235	205.8	0.95
57	4150	830	29.00	235	205.8	0.97
58	4150	830	28.50	235	205.8	0.98
59	4150	830	27.50	235	205.8	1.02
60	4150	830	27.00	235	205.8	1.04
61	4150	830	26.50	235	205.8	1.06
62	4150	830	26.00	235	205.8	1.08
63	4150	830	25.50	235	205.8	1.10
64	4150	830	25.00	235	205.8	1.12
65	4150	830	24.50	235	205.8	1.14
66	4150	830	24.00	235	205.8	1.17
67	4150	830	23.50	235	205.8	1.19
68	4150	830	23.00	235	205.8	1.22
69	4150	830	22.50	235	205.8	1.25
70	4150	830	22.00	235	205.8	1.27
71	4150	830	21.50	235	205.8	1.30
72	4150	830	21.00	235	205.8	1.34
73	4150	830	20.50	235	205.8	1.37
74	4150	830	20.00	235	205.8	1.40
75	4150	830	19.50	235	205.8	1.44
76	4150	830	19.00	235	205.8	1.48
77	4150	830	18.50	235	205.8	1.52
78	4150	830	18.00	235	205.8	1.56
79	4150	830	17.50	235	205.8	1.60
80	4150	830	17.00	235	205.8	1.65
81	4150	830	16.50	235	205.8	1.70
82	4150	830	16.00	235	205.8	1.75
83	4150	830	15.50	235	205.8	1.81
84	4150	830	15.00	235	205.8	1.87
85	4150	830	14.50	235	205.8	1.93
86	4150	830	14.00	235	205.8	2.00
87	4150	830	13.50	235	205.8	2.08
88	4150	830	13.00	235	205.8	2.16
89	4150	830	12.50	235	205.8	2.24
90	4150	830	12.00	235	205.8	2.34
91	4150	830	11.50	235	205.8	2.44
92	4150	830	11.00	235	205.8	2.55
93	4150	830	10.50	235	205.8	2.67
94	4150	830	10.00	235	205.8	2.80
95	4150	830	9.50	235	205.8	2.95
96	4150	830	9.00	235	205.8	3.12
97	4150	830	8.50	235	205.8	3.30
98	4150	830	8.00	235	205.8	3.51
99	4150	830	7.50	235	205.8	3.74
100	4150	830	7.00	235	205.8	4.01

Once the best-fit PDF is selected from the A-D test, it is requested to decide the best-interval of histogram which can be calculated from the value satisfying the maximum mean and minimum COV as shown in Fig. 6. The best-fit PDF with histogram can then be plotted together as shown in Fig. 7.

In this study, plate slenderness ratio (β) is set as a reference parameter. In addition, fixed mean values of plate length (= 4,150mm) and breadth (= 830mm) which gives representative half-wave number (m) of 5 were adopted from Fig. 6(a) and (b). In the case of material yield strength, two representative values such as 235MPa (Mild steel, MS24) and 315MPa (High tensile steel, HT32) were used. In the case of PDF of plate slenderness ratio, 3-Parameter Loglogistic function was selected for the best-fit PDF based on the Anderson-Darling test as shown in Fig. 6(d) and Table 1.

One hundred (100) cases of reliable plate scenarios were selected based on the calculation of area under PDF of plate slenderness ratio as presented in Fig. 2(d). Once an expected number of β is selected, plate thickness can be recalculated. In this process, β values can slightly be adjusted due to limitation of thickness based on product standard available in the industry. The selected plate scenarios are summarized in Table 2.

3.3. Calculation of ultimate strength for selected scenarios

The ultimate strength analysis was conducted by ANSYS nonlinear FE simulation code for the selected reliable plate scenarios. In the modelling of the plate, there are few things to be considered such as effect of boundary condition, range of model (= model size), initial imperfections, applied loading, and many others. All those important considerations should be confirmed before FE simulation is conducted. Previously, a number of studies have been conducted to determine reliable range of the plate modelling by FEM (ISSC 2012, 2015) In this study, one - bay and one-span plate model is adopted for FE simulation.

Figures 8(a) and (b) show applied plate initial deflection and boundary conditions, respectively. In Fig. 8(a), agreement between applied initial deflection formulation in Eq. (3) and node coordinates in FE model are compared. Those two were perfectly matched which means that the geometry of initially deflected plate is well-modelled. Based on the mesh convergence study in Fig. 8(b), 0.1 of mesh size and plate breadth ratio was selected for the numerical simulation.

This plate (or unstiffened panel) is considered as the main structural component of ships and offshore structures together with stiffener structures. For the safe design of plate, simply supported boundary condition is assumed in this study to produce maximum deflection of the plate with higher stress values for the pessimistic design. In the case of a model range, one-bay and one-span plate model surrounded by longitudinal stiffener and transverse frames are adopted based on ISSC (2012).

During the fabrication, initial imperfection naturally occurs in steel structure, especially for initial deflection and welding-induced residual stress which are taken into account in the ship and offshore construction. In this study, three different levels of initial deflection which includes slight level ($C_{ID} = 0.025$), average level ($C_{ID} = 0.10$) and severe level ($C_{ID} = 0.30$), proposed by Smith *et al.* (1988), were considered as illustrated in Eq. (4). For the research purpose, additional four initial deflection coefficients (C_{ID} = 0.05, 0.15, 0.20 and 0.25) were also considered. In total, seven (7) C_{ID} values were applied to identify the effect of initial deflection on the ultimate strength of plate element which will be covered in the next section. A typical example of the ultimate strength analysis result (Scenario No. 31) is presented in Fig. 8(c).

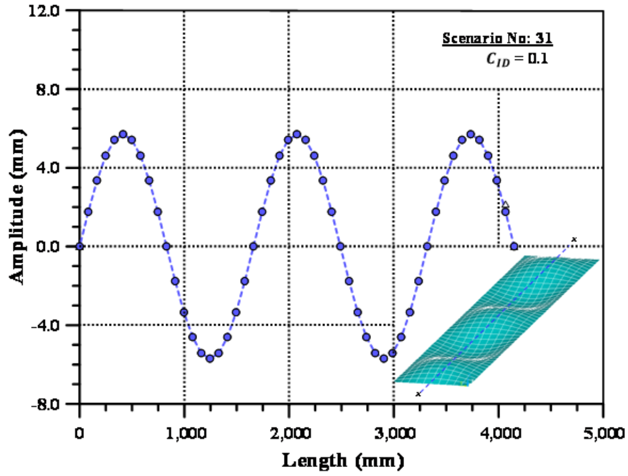

(a) Initial deflection

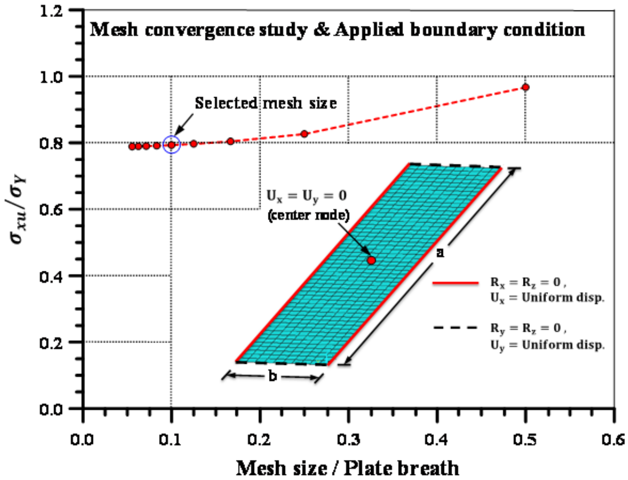

(b) boundary condition & mesh size

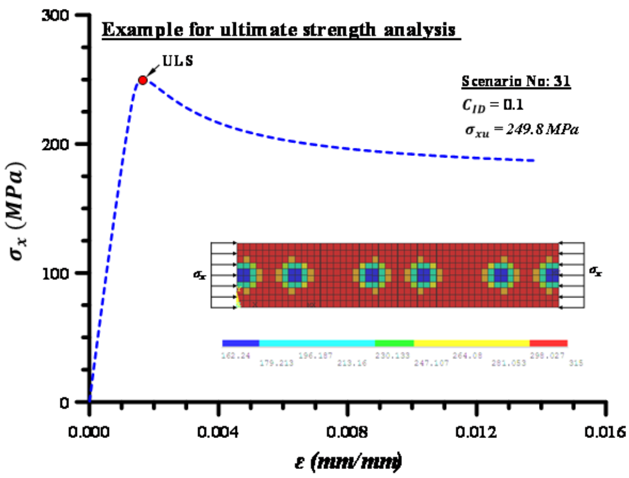

(c) ultimate strength analysis

Fig.8 Typical example of FE modelling and verification

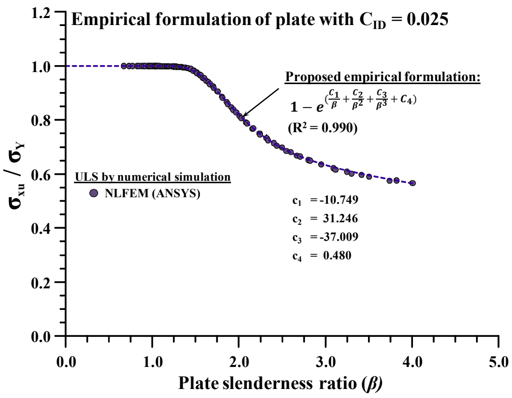

(a) C_{ID} = 0.025 (slight level)

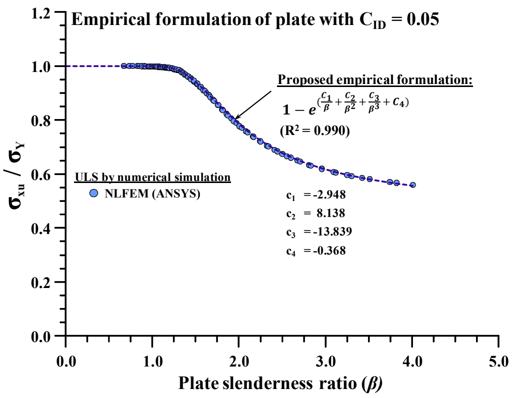

(b) C_{ID} = 0.05

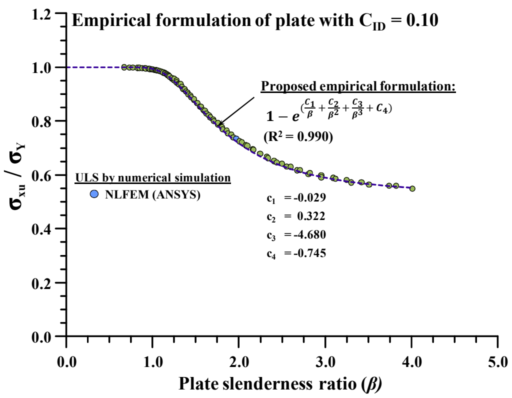

(c) C_{ID} = 0.1 (average level)

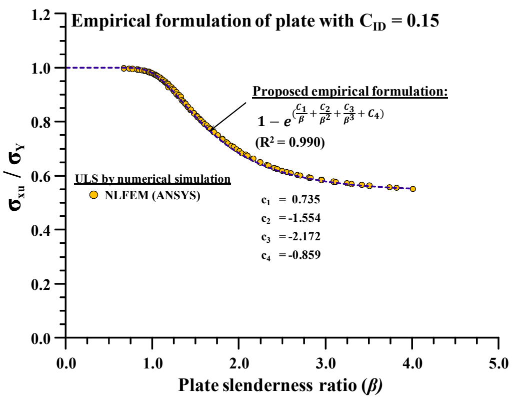

(d) C_{ID} = 0.15

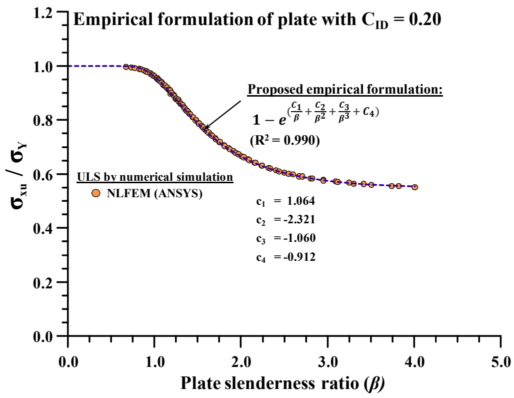

(e) C_{ID} = 0.20

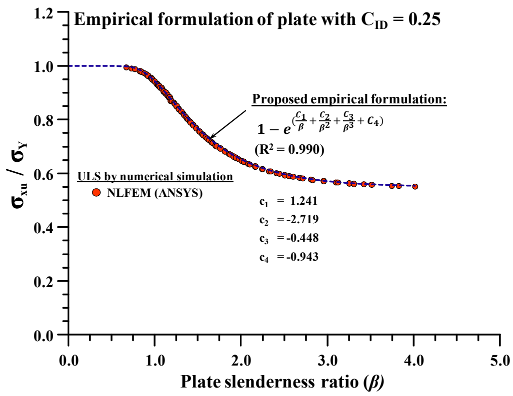

(f) C_{ID} = 0.25

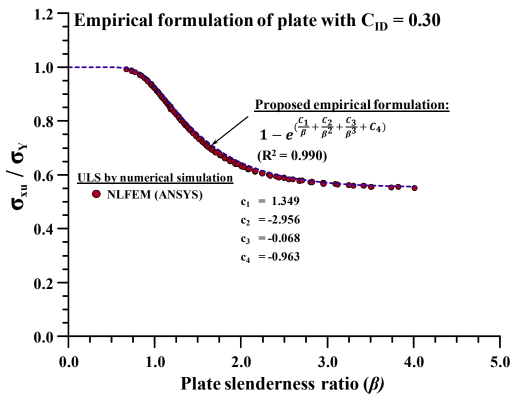

(g) C_{ID} = 0.30 (severe level)

Fig.9 Developed empirical formulation

Once numerical simulations are done by the ANSYS NLFEM for selected seven hundred (700) plate scenarios, it can be plotted in the relationship between plate slenderness ratio versus ultimate strength performance as shown in Fig. 9. It is well presented that all of the cases show good-agreement with proposed formulation (R^2 = 0.99). In the figure, the proposed empirical formulation is also presented together with determined sub-coefficients of IDI such as c_1, c_2, c_3, and c_4 as illustrated in Eq. (2) and Figs. 9(a) to (g). Details may be referred in the next section.

3.4. Identification of initial deflection effect on ultimate strength of plate

Once plate is collected, the structure characteristics can be analysed in terms of geometrical properties (plate length, plate breadth, plate thickness) and material properties (Elastic modulus, Poisson's ratio, Yield strength, Ultimate strength, etc.) for the modelling of the plate element.

Once calculations of ultimate strength for the selected scenarios are finished, the effect of initial deflection on ultimate strength of plate element can be identified. Figure 10 shows obtained best-fit empirical formulation based on numerical simulation results by ANSYS NLFEM. As expected, the effect of initial deflection could be expressed by Eq. (1) and those obtained equations showed good agreement with analysis results (R^2 = 0.99) as shown in Fig. 9.

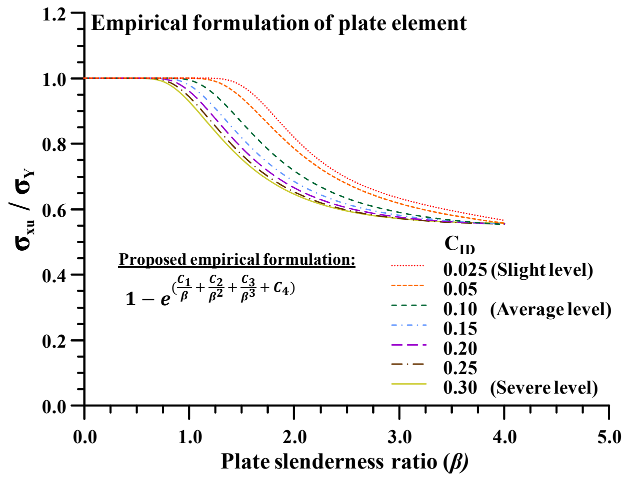

Fig.10 Numerical simulation results with obtained best-fit lines (C_1 - C_4 values can be referred to Table 3)

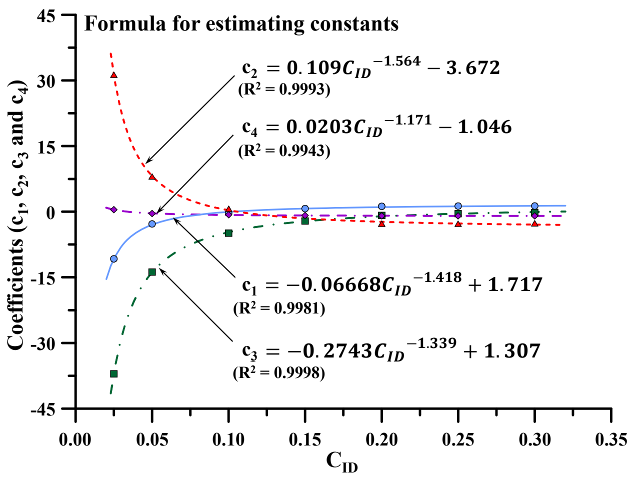

Fig.11 Relationship between C_{ID} and sub-coefficients for the identification of initial deflection effect

In order to predict the ultimate strength of plate with other values of initial deflection coefficient (C_{ID}), relationship between C_{ID} and sub-coefficients of IDI (c_1 , c_2 , c_3 , c_4) were investigated in Fig. 11. This may be considered as the highlight of this study. It means that prediction of ultimate strength of initially deflected plate can be done by simplified empirical formulation based on the following procedure.

[Step 1] Determine C_{ID} value based on (1) measurement, or (2) assumption based on historical data.
[Step 2] Calculate sub-coefficients (c_1 , c_2 , c_3 , and c_4) by following Eq. (2) and Table 4.
[Step 3] Calculate initial deflection index from Eq. (1).
[Step 4] Prediction of ultimate strength of plate by proposed empirical formulation in Eq. (5).

Table 3 Obtained sub-coefficients of IDI from Fig. 9

C_{ID}	c_1	c_2	c_3	c_4
0.025	-10.749	31.246	-37.009	0.480
0.05	-2.948	8.138	-13.839	-0.368
0.10	-0.029	0.322	-4.680	-0.745
0.15	0.735	-1.554	-2.172	-0.859
0.20	1.064	-2.321	-1.060	-0.912
0.25	1.241	-2.719	-0.448	-0.943
0.30	1.349	-2.956	-0.068	-0.963

Table 4 Relationship between C_{ID} and sub-coefficients of initial deflection index (IDI)

$c_{i,\ i=1\ to\ 4} = \omega (C_{ID})^{\xi} + \psi$ from Eq. (2)	c_1	c_2	c_3	c_4
ω	-0.06668	0.1090	-0.2743	0.0203
ξ	-1.418	-1.564	-1.339	-1.171
ψ	1.717	-3.672	1.307	-1.046
R^2	0.9981	0.9993	0.9998	0.9943

3.5. Development of advanced empirical formulation & verification

Once advanced empirical formulation is developed, verification with numerical analysis result may be required to determine its reliability. Fig. 12 shows comparison of results between calculated ultimate strength performance by ANSYS NLFEM and obtained results by proposed empirical formulation. Mean and coefficient of variation (COV) values are also presented for seven (7) cases of initial deflections as considered for our calculation.

In case of mean and COV values, it shows nearly 1.0 and 0.0, in respectively. It means that proposed empirical formulation can be considered as reliable solution and numerical simulation can be replaced by proposed empirical formulation with effective computation cost.

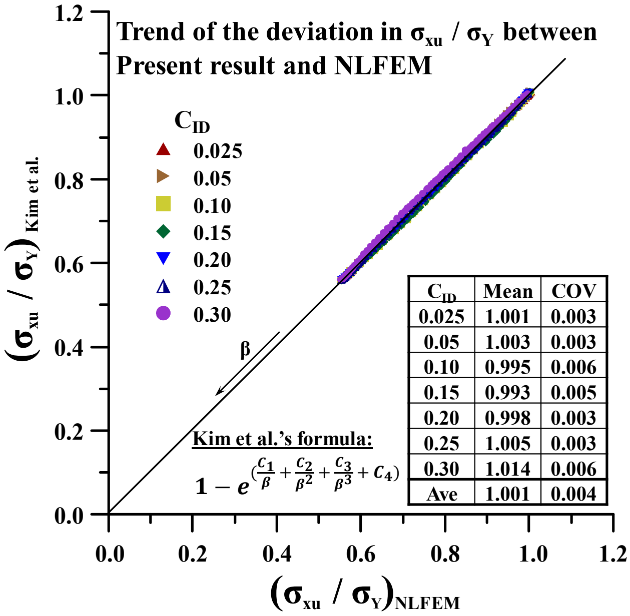

Fig.12 Trend of the deviation in ultimate strength of plate between proposed empirical formulation and ANSYS nonlinear finite element method (NLFEM)

4. Concluding remarks

In this study (Part I), an advanced empirical formulation was proposed by applying the initial deflection index (IDI) concept to predict the ultimate strength performance of plate under longitudinal compression. The proposed concept and whole procedure to develop advanced empirical formulation were verified by numerical simulations conducted by the ANSYS nonlinear FEM for seven hundred (700) selected plate scenarios. The obtained empirical formulation was well-fitted with all of the numerical simulation results (R^2= 0.99) and will be useful for structural engineers to predict ultimate strength behaviour of the plate element.

In the case of initial deflection of the plate, basically three different levels such as slight, average, and severe were considered and general trends were formulated to predict other values of initial deflection. Other types of plate range and boundary condition may be considered for further study. In Part II, historical review and detailed benchmark study of the plate element will be conducted based on the comparison between obtained FE results and existing design and empirical formulations.

Acknowledgements

The authors would also like to thank for the technical support by POSTECH, POSCO, and Daewoo E &C, Republic of Korea. The authors would like to thank Daewoo E&C, POSTECH, and POSCO in the Republic of Korea for their kind support. This research was supported by the Technology Innovation Program (Grant No.: 10053121) funded by the Ministry of Trade, Industry & Energy (MI, Korea). Some part of the study was presented in The 3rd international conference on civil offshore & environmental engineering (ICCOEE 2016), from 15-17 August 2016 in Kuala Lumpur, Malaysia.

References

AISC (1964), *Specification for the design, fabrication and erection of structural steel for buildings*, American Institute of Steel Construction; Chicago, IL, USA.

ANSYS (2014), *User's manual version 13.0*, ANSYS Inc., Canonsburg, PA, USA.

Bortsch, R. (1921), "Die mitwirkende Plattenbreite", *Der Bauingenieur*, **23**, 662-667 (in German).

Box, T. (1883), *A practical treatise on the strength of materials: Including their elasticity and resistance to impact*, E. & F.N. Spon, London, UK.

BS 153 (1966), *Steel Girder Bridges, Part 4, Design and Construction*, British Standards Institution; London, UK.

BS 499 (1961), *The use of structural steel in building and Addendum*, British Standards Institution; London, UK.

Carlsen, C.A. (1977), "Simplified collapse analysis of stiffened plates", *Norwegian Maritime Research*, **7**(4), 2-36.

Cerik, B.C. (2018), "Ultimate longitudinal compressive strength of steel plates with lateral patch load induced plastic deformation", *Thin-Walled Structures*, **122**, 416-424.

Chilver, A.H. (1953), "The maximum strength of the thin-walled channel strut", *Civil Engineering and Public Works Review*, **48**, 1143-1146.

Cox, H.L. (1933), "Buckling of thin plates in compression", *R&M No. 1554*, British Aeronautical Research Committee (ARC), UK.

Cui, W. and Mansour, A.E. (1998), "Effects of welding distortions and residual stresses on the ultimate strength of long rectangular plates under uniaxial compression", *Marine Structures*, **11**(6), 251-269.

Czujko, J. and Paik, J.K. (2015), "A new method for accidental limit states design of thin walled structures subjected to hydrocarbon explosion loads", *Ships and Offshore Structures*, **10**(5), 460-469.

DNV (1987), *Use of high tensile steel in ship structures*, The Tanker Structure Co-operative Forum Meeting with Shipbuilders, Det Norske Veritas, Paramus, NJ, USA.

Dow, R.S. and Smith, C.S. (1984), "Effects of localized imperfections on compressive strength of long rectangular plates", *Journal of Constructional Steel Research*, **4**, 51-76.

Dwight, J.B. and Moxham, K.E. (1969), "Welded steel plates in compression", *The Structural Engineer*, **47**(2), 49-66.

Faulkner, D. (1975), "A review of effecting plating for use in analysis of stiffened plating in bending and compression", *Journal of Ship Research*, **19**(1), 1-17.

Frankland, J.M. (1940), "The Strength of Ship Plating Under Edge Compression. U.S.", *Experimental Model Basin Progress Report 469*.

Gerard, G. (1957), "Part 4 – Failure of plates and composite elements", *Handbook of structural stability, NACA TN 3784*.

Gordon, J.M., Teixeira, A.P. and Guedes Soares, C. (2011), "Ultimate strength of ship structures", Edited by Guedes Soares C, Garbatov Y, Teixeira AP editors, *Marine Technology and Engineering*, Taylor & Francis Group, London, UK.

Guedes Soares, C. (1988), "Design equations for the compressive strength of unstiffened plate elements with initial imperfections", *Journal of Constructional Steel Research*, **9**(4), 287-310.

Guedes Soares, C., Gordo, J.M. and Teixeira, A.P. (2000), "Design equations for plate subjected to heat loads and lateral pressure", *Marine Structures*, **13**(1), 1-23.

Hogstrom, P. and Ringberg, J.W. (2012), "An extensive study of a ship's survivability after collision – a parameter study of material characteristics, non-linear FEA and damage stability analyses", *Marine Structures*, **27**(1), 1-28.

Hong, L. and Amdahl, J. (2012), "Rapid assessment of ship grounding over large contact surface", *Ships and Offshore Structures*, **7**(1), 5-19.

Hughes, O.F. (1983), *Ship Structural Design: A Rationally-Based, Computer-Aided Optimization Approach*, Wiley, New York, NY, USA.

ISSC (2012), "Ultimate Strength (Committee III.1)", *The 18th International Ship and Offshore Structures Congress (ISSC 2012)*, 9-13 September, Rostock, Germany.

ISSC (2015), "Ultimate Strength (Committee III.1)", *The 19th International Ship and Offshore Structures Congress (ISSC 2015)*, 7-10 September, Cascais, Portugal.

Ivanov, L.D. and Rousev, S.H. (1979), "Statistical estimation of reduction coefficient of ship's hull plates with initial deflections", *The Naval Architect*, **4**, 158-160.

Jiang, X.L., Yu, H.Y. and Kaminski, M.L. (2014), "Assessment of residual ultimate hull girder strength of damaged ships", The *33rd International Conference on Ocean, Offshore and Arctic Engineering (OMAE2014)*, San Francisco, CA, USA (OMAE2014-23153).

John, W. (1987), "On the strains of iron ships", *RINA Transactions*, **18**, 98-117.

Kim, D.K., Kim, B.J., Seo, J.K., Kim, H.B., Zhang, X.M. and Paik, J.K. (2014), "Time-dependent residual ultimate longitudinal strength - grounding damage index (R-D) diagram", *Ocean Engineering*, **76**, 163-171.

Kim, D.K., Kim, H.B., Mohd, M.H. and Paik, J.K. (2013a), "Comparison of residual strength-grounding damaged index diagrams for tankers produced by the ALPS/HULL ISFEM and design formula method", *International Journal of Naval Architecture and Ocean Engineering*, **5**(1), 47-61.

Kim, D.K., Lim, H.L., Kim, M.S., Hwang, O.J. and Park, K.S. (2017), "An empirical formulation for predicting the ultimate strength of stiffened panels subjected to longitudinal compression", *Ocean Engineering*, **140**, 270-280.

Kim, D.K., Lim, H.L. and Yu, S.Y. (2018a), "A technical review on ultimate strength prediction of stiffened panels in axial compression", *Ocean Engineering*, Under revision.

Kim, D.K., Ng, W.C.K. and Hwang, O.J. (2018b), "An empirical formulation to predict maximum deflection of blast wall under explosion", *Structural Engineering and Mechanics*, Accepted for publication.

Kim, D.K., Ng, W.C.K. Hwang, O.J., Sohn, J.M. and Lee, E.B. (2018c), "Recommended finite element formulations for the analysis of offshore blast walls in an explosion", *Latin American Journal of Solids and Structures*, Accepted for publication.

Kim, D.K., Park, D.K., Kim, J.H., Kim, S.J., Kim, B.J., Seo, J.K. and Paik, J.K. (2012a), "Effect of corrosion on the ultimate strength of double hull oil tankers – Part I: stiffened panels", *Structural Engineering and Mechanics*, **42**(4), 507-530.

Kim, D.K., Park, D.K., Park, D.H., Kim, H.B., Kim, B.J., Seo, J.K. and Paik, J.K. (2012b), "Effect of corrosion on the ultimate strength of double hull oil tankers – Part II: hull girders", *Structural Engineering and Mechanics*, **42**(4), 531-549.

Kim, D.K., Perdersen, P.T., Paik, J.K., Kim, H.B., Zhang, X.M. and Kim, M.S. (2013b), "Safety guidelines of ultimate hull girder strength for grounded container ships", *Safety Science*, **59**, 46-54.

Kim, D.K. and Poh, B.Y. (2018), "Ultimate strength of initially deflected plate under longitudinal compression: Part II = Reviews on accuracy of existing formulations", *Structural Engineering and Mechanics*, Under review.

Kim, D.K., Yu, S.Y. and Choi, H.S. (2013c), "Condition assessment of raking damaged bulk carriers under vertical bending moments", *Structural Engineering and Mechanics*, **46**(5), 629-644.

Marguerre, K. (1937), "Die mittragende breite der gedruckten platte", Translated *NACA Technical Note 833* (in German) (original in *Luftfahrt Forschung*, **14**(3), 121).

Metzer, W. (1929), "Die mittragende Breite", Dissertation, *der Technischen Hochschule zu Aache* (in German).

Ozdemir, M., Ergin, A., Yanagihara, D., Tanaka, S. and Yao, T. (2018), "A new method to estimate ultimate strength of stiffened panels under longitudinal thrust based on analytical formulas", *Marine Structures*, **59**, 510-535.

Paik, J.K. (2018), *Ultimate limit state analysis and design of plated structures*: Second Edition, Jon Wiley & Sons, Chichester, UK.

Paik, J.K., Kim, B.J., Jeong, J.S., Kim, S.H., Jang, Y.S., Kim, G.S., Woo, J.H., Kim, Y.S., Chun, M.J., Shin, Y.S. and Czujko, J. (2010), "CFD simulation of gas explosion and fire actions", *Ships and Offshore Structures*, **5**(1), 3-12.

Paik, J.K., Kim, B.J. and Seo, J.K. (2008a), "Methods for ultimate limit state assessment of ships and ship-shaped offshore structures: Part I Unstiffened plates", *Ocean Engineering*, **35**(2), 261-270.

Paik, J.K., Kim, B.J. and Seo, J.K. (2008b), "Methods for ultimate limit state assessment of ships and ship-shaped offshore structures: Part II Stiffened panels", *Ocean Engineering*, **35**(2), 271-280.

Paik, J.K., Kim, B.J. and Seo, J.K. (2008c), "Methods for ultimate limit state assessment of ships and ship-shaped offshore structures: Part III Hull girders", *Ocean Engineering*, **35**(2), 281-286.

Paik, J.K., Kim, D.K., Park, D.H., Kim, H.B. and Kim, M.S. (2012), "A new method for assessing the safety of ships damaged by grounding", *International Journal of Maritime Engineering*, **154**(A1), 1-20.

Paik, J.K., Kim, D.K., Park, D.H., Kim, H.B., Mansour, A.E. and Caldwell, J.B. (2013), "Modified Paik-Mansour formula for ultimate strength calculations of ship hulls", *Ships and Offshore Structures*, **8**(3-4), 245-260.

Paik, J.K., Lee, J.M. and Lee, D.H. (2003), "Ultimate strength of dented steel plates under axial compression loads", *International Journal of Mechanical Sciences*, **45**(3), 433-448.

Paik, J.K., Thayamballi, A.K. and Lee, J.M. (2004). "Effect of initial deflection shape on the ultimate strength behavior of welded steel plates under biaxial compressive loads", *Journal of Ship Research*, **48**(1), 45-60.

Paik, J.K., Thayamballi, A.K. and Yang, S.H. (1998), "Residual strength assessment of ships after collision and grounding", *Marine Technology*, **35**(1), 38-54.

Park, D.K., Kim, D.K., Seo, J.K., Kim, B.J., Ha, Y.C. and Paik, J.K. (2015a), "Operability of non-ice glass aged ships in the Arctic Ocean – Part I: Ultimate limit state approach", *Ocean Engineering*, **102**, 197-205.

Park, D.K., Kim, D.K., Seo, J.K., Kim, B.J., Ha, Y.C. and Paik, J.K. (2015b), "Operability of non-ice glass aged ships in the Arctic Ocean – Part II: Accidental limit state approach", *Ocean Engineering*, **102**, 206-215.

Raviprakash, A.V., Prabu, B. and Alagumurthi, N. (2012), "Residual ultimate compressive strength of dented square plates", *Thin-Walled Structures*, **58**, 32-39.

Saad-Eldeen, S., Garbatov, Y. and Guedes Soares, C. (2016), "Ultimate strength analysis of highly damaged plates", *Marine Structures*, **45**, 63-85.

Schnadel, G. (1930), "Die uberschreitung der knickgrenze dunnen platen", *Proceedings of the 3rd International Congress on Applied Mechanics*, pp. 73 (See DTMB translation 66, 1950), Stockholm, Sweden.

Schuman, L. and Back, G. (1930), "Strength of rectangular flat plates under edge compression", *NACA Technical Report 356*, National Advisory Committee for Aeronautics, Washington, DC, USA.

Sechler, E.E. (1933), *The ultimate strength of thin flat sheets in compression*, Guggenheim Aeronautical Laboratory Publication 27, California Institute of Technology, Pasadena, CA, USA.

Smith, C.S., Davidson, P.C., Chapman, J.C. and Dowling, P.J. (1988), "Strength and stiffness of ship's plating under in-plane compression and tension", *Tran RINA*, **130**, 277-296.

Sohn, J.M., Kim, S.J., Kim, B.H. and Paik, J.K. (2013), "Nonlinear structural consequence analysis of FPSO topside blastwalls", *Ocean Engineering*, **60**, 149-162.

Soreide, T.H. and Czujko, J. (1983), "Load-carrying capacity of plates under combined lateral load and axial/biaxial compression", The *2nd International Symposium on Practical Design in Shipbuilding*, Tokyo, Japan.

Teixeira, A.P., Ivanov, L.D. and Guedes Soares, C. (2013), "Assessment of characteristics values of the ultimate strength of corroded steel plates with initial imperfections", *Engineering Structures*, **56**, 517-527.

Timoshenko, S. (1936), *Theory of Elastic Stability*: First Edition, McGraw Hill, New York, NY, USA.

Ueda, Y., Yao, T., Nakacho, K. and Yuan, M.G. (1992), *Prediction of welding residual stress, deformation and ultimate strength of plate panels*, Engineering Design in Welded Constructions, Pergamon Press, Oxford, UK.

Ueda, Y., Yasukawa, W., Yao, T., Ikegami, H. and Ominami, R. (1975), "Ultimate strength of square plates subjected to compression effects of initial deflection and welding residual stresses (1st report)", *J. Soc. Naval Architects of Japan*, **137**, 210-221.

von Karman, T. (1924), "Die mittragende Breite (The effective width), *Beitrage zur technischen Mechanik* (in German).

Wijaya, C. and Kim, B.T. (2011), "FE analysis of unstiffened and stiffened corrugated panels subjected to blast loading", *Journal of Mechanical Science and Technology*, **25**(12), 3159-3164.

Winter, G. (1940), "Stress distribution in and equivalent width of flanges of wide thin-wall steel beams", *NACA Technical, Note 784*.

Witkowska, M. and Guedes Soares, C. (2015), "Ultimate strength of locally damaged panels", *Thin-Walled Structures*, **97**, 225-240.

Xu, M.C. and Guedes Soares, C. (2013), "Assessment of residual ultimate strength for side dented stiffened panels subjected to compressive loads", *Engineering Structures*, **49**, 316-328.

Xu, M.C. and Guedes Soares, C. (2015), "Effect of a central dent on the ultimate strength of narrow stiffened panels under axial compression", *International Journal of Mechanical Sciences*, **100**, 68-79.

Yao, T. and Fujikubo, M. (2016), *Buckling and Ultimate Strength of Ship and Ship-like Floating Structures*, Elsevier Inc., New York, USA.

Youssef, S.A.M., Faisal, M., Seo, J.K., Kim, B.J., Ha, Y.C., Kim, D.K., Paik, J.K., Cheng, F. and Kim, M.S. (2016), "Assessing the risk of ship hull collapse due to collision", *Ships and Offshore Structures*, **11**(4), 335-350.